HHS Public Access

Author manuscript

Biosens Bioelectron. Author manuscript; available in PMC 2020 April 01.

Published in final edited form as:

Biosens Bioelectron. 2019 April 01; 130: 338–343. doi:10.1016/j.bios.2018.09.050.

Quantification of cDNA on GMR biosensor array towards point-of-care gene expression analysis

Neeraja Ravi[a,*], **Giovanni Rizzi**[b], **Sarah E. Chang**[c,d], **Peggie Cheung**[c,d], **Paul J. Utz**[c,d], and **Shan X. Wang**[b,e]

[a]Department of Bioengineering, Stanford University, Stanford, CA 93405, USA

[b]Department of Materials Science and Engineering, Stanford University, Stanford, CA 93405, USA

[c]Institute for Immunity, Transplantation and Infection, Stanford University School of Medicine, Stanford, CA 94305, USA

[d]Department of Medicine, Division of Immunology and Rheumatology, Stanford University School of Medicine, Stanford, CA 94305, USA

[e]Department of Electrical Engineering, Stanford University, Stanford, CA 93405, USA

Abstract

Gene expression analysis at the point-of-care is important for rapid disease diagnosis, but traditional techniques are limited by multiplexing capabilities, bulky equipment, and cost. We present a gene expression analysis platform using a giant magnetoresistive (GMR) biosensor array, which allows multiplexed transcript detection and quantification through cost-effective magnetic detection. In this work, we have characterized the sensitivity, dynamic range, and quantification accuracy of Polymerase chain reaction (PCR)-amplified complementary DNA (cDNA) on the GMR for the reference gene GAPDH. A synthetic GAPDH single-stranded DNA (ssDNA) standard was used to calibrate the detection, and ssDNA dilutions were qPCR-amplified to obtain a standard curve. We demonstrate that the GMR platform provides a dynamic range of 4 orders of magnitude and a limit of detection of 1 pM and 0.1 pM respectively for 15 and 18-cycle amplified synthetic GAPDH PCR products. The quantitative results of GMR analysis of cell-line RNA were confirmed by qPCR.

[*]Corresponding Author: 476 Lomita Mall, Stanford, CA, 94305, Tel.: (925) 413-2825.
neravi@stanford.edu, grizzi@stanford.edu, sechang@stanford.edu, pcheung@stanford.edu, pjutz@stanford.edu, sxwang@stanford.edu

Disclosures

The authors declare the following competing financial interest(s): S.X.W. have related patents or patent applications assigned to Stanford University and out-licensed for potential commercialization. S.X.W. has stock or stock options in MagArray, Inc., which has licensed relevant patents from Stanford University for commercialization of GMR nanosensor chips.

Keywords

GMR sensors; PCR; gene expression; DNA melting; array; point-of-care

1. Introduction

Many gene expression profiles have been used to detect the presence and monitor the progression of diseases, such as cardiovascular disease (Elashoff et al., 2011), tuberculosis (Maertzdorf et al., 2016), and influenza (Andres-Terre et al., 2015). These signatures measure gene regulation compared to the healthy state, and involve the simultaneous measurement of both high and low abundance transcripts. Therefore, there is a need for diagnostic technologies that can accurately quantify transcript concentration for a particular gene in real-time.

The gold standard for gene expression analysis is quantitative reverse transcription PCR (RT-qPCR), in which amplification is measured in real-time from an RNA sample of interest. However, qPCR is limited in multiplexing capabilities, as only a certain amount of filters are present to detect different fluorophore fluorescence (Dobnik et al., 2016). More recently, next generation sequencing (NGS) has become prevalent for high throughput gene expression analysis. While this is a good discovery tool to search for potential gene targets, the high cost, complex equipment, and time to get results render it impractical for rapid and targeted differential expression analysis for a limited number of genes (Arts et al., 2017).

We propose giant magnetoresistive (GMR) sensors as a targeted gene expression analysis platform. Previously, these devices have been shown to detect proteins, like cancer biomarkers (Gaster et al., 2009), autoantibodies (Lee et al., 2016), and common allergens (Ng et al., 2016), with high sensitivity and specificity. They have also been utilized for DNA detection (Xu et al., 2008), and have been well characterized for simultaneous mutation and methylation analysis (Rizzi et al., 2017). GMR sensors function through localized proximity magnetic sensing. Magnetic nanoparticles can be used as tags on DNA to generate a magnetic field that is detected by the GMR sensor; in this way, binding of DNA to the sensor surface can be detected in real time (Osterfeld et al., 2008). Advantages of magnetic sensing compared to traditional optical biomolecule detection include a lower limit of detection, higher dynamic range, temperature insensitivity, and lower background levels in biological samples (Xu et al., 2008; Rizzi et al., 2017). Importantly, because the GMR chip has 80 different sensors, the device is robust to multiplexing compared to other platforms.

Gene expression analysis using GMR sensors relies on hybridization-based detection; in which GMR chips are spotted with single strand DNA (ssDNA) probes complementary to the gene of interest. Total mRNA is isolated and reverse transcribed with primers corresponding to the gene of interest to create double-stranded cDNA. Upon denaturation, the single-stranded cDNA is applied to the sensor and allowed to hybridize to the probes. In this sense, the GMR platform is quite similar to the microarray for gene expression analysis (Allison et al., 2006), but melt curve analysis can also be performed with the GMR system to further increase hybridization specificity. Moreover, the GMR system has been developed into a portable, low cost device (Choi et al., 2016), enabling clinical diagnostics at the point-

of-care. To prevent cross-contamination between samples, the GMR chips are not reused; this is unproblematic because GMR chips are relatively inexpensive (each chip is roughly $2–3).

It has been shown that the GMR sensor platform had a dynamic detection range of 40 pM to 40 nM for non-amplified synthetic ssDNA (Rizzi et al., 2017). However, there has not been extensive characterization of the sensitivity, dynamic range, and quantification accuracy of PCR-amplified DNA on the GMR for varying PCR cycle numbers. Coupled with the multiplexing capabilities of the GMR, this is important to ensure that multiple transcripts can simultaneously be detected and quantified in a broad concentration range. In this work, we have characterized the GMR sensor platform for cDNA detection and quantification. We have demonstrated that the GMR is a strong endpoint detection technology to measure levels of cDNA, and has the potential to be applied to detect disease signatures at the point-of-care.

2. Material and Methods

2.1 RNA Extraction and Reverse Transcription.

HeLa cells (line S3) were seeded into 10cm dishes around 50–60% confluency. Afterwards, HeLa cell mRNA was extracted using the Qiagen RNeasy Mini Kit according to their protocol. cDNA was synthesized using Invitrogen's Superscript III First Strand Synthesis System according to their protocol.

2.2 qPCR Amplification.

Prior to GMR detection, HeLa cDNA was qPCR-amplified (BioRad CFX96 Real-Time System) with primers spanning two GAPDH exons. We chose GAPDH expression as a test case, since it is a common reference gene for qPCR (Kozera and Rapacz, 2013). A synthetic target ssDNA was used as a standard to calibrate the detection. The sequence of the standard corresponded to the amplicon obtained from GAPDH primers, originally in a 100 μM stock diluted to a 100 nM solution. All sequences can be found in supplementary material Table S1 (Integrated DNA Technologies). The primers had a stock concentration of 100 μM and were diluted to 10 μM prior to use. Sso Advanced Universal SYBR Grn Suprmix (Bio-rad) was used for fluorescence detection, and a master mix was created with 1:5 dilution of Supermix to primers. The total volume of each qPCR reaction was 10 μL, with 1 μL of target DNA, 7 μL of master mix, and 2 μL of DNA suspension buffer (Teknova). PCR amplification was initiated with polymerase activation and DNA denaturation at 95°C for 30 seconds, followed by 40 cycles with denaturation at 95°C for 10 seconds, and annealing and extension at 61°C for 30 seconds. A melting ramp was performed (65–95°C) at the end of the 40 cycles to assess primer specificity.

2.3 qPCR standard curve.

A dilution series of a synthetic target ssDNA with sequence corresponding to the amplicon obtained from GAPDH primers was measured with qPCR as described above. ssDNA was diluted in a 10-fold dilution series, from 10 nM to 0.1 pM. Each subsequent concentration was amplified to saturation through a 40 cycle PCR reaction. Samples for each concentration were run in duplicate, and each intensity value on the curve was normalized to the intensity

value at 40 cycles and averaged. The Cq values of the standard dilutions were extracted and plotted to create a standard curve using Bio-Rad CFX Maestro software.

2.4 GMR Sensor Preparation.

The GMR biosensor arrays comprised of 8×10 sensors were fabricated as described previously (Osterfeld et al., 2008). The sensors are functionalized with amino-modified DNA probes using a surface silanization. Briefly, the surface was activated with a 15-min treatment with 15% Hydrogen Peroxide (Certified ACS, Sigma-Aldrich) in distilled water, 30-min treatment with 10% (3-Aminopropyl) triethoxysilane (Sigma Aldrich) in acetone, 30 min treatment with 5% Glutaraldehyde (Fisher Scientific) in distilled water, and a final wash with distilled water. The amino-modified DNA probes (sequences in Supplementary Table S1) were spotted (~1.5 nL) onto separate sensors of the GMR chip using a robotic arrayer (sciFlexarrayer, Scienion) according to the pattern seen in Fig. 1. Each DNA probe was diluted to 20 μM in filtered 2x saline sodium citrate SSC (Invitrogen) from a stock solution of 20x SSC prior to spotting. A total of 32 sensors were functionalized with the probe complementary to GAPDH, 12 sensors were functionalized with a DNA sequence non-complementary to the PCR amplified product as negative control, and 12 sensors were functionalized with biotinylated DNA as positive control. The chips were stored at room temperature until use. Prior to use, the GMR chips were inserted into cartridges defining a reaction well over the sensors. The chip surface was then washed and blocked with 1% BSA in PBS as described previously (Osterfeld et al., 2008) to prevent non-specific binding.

2.5 Pre-PCR dilution series.

The sensor signal vs. PCR product concentration was characterized by measuring a dilution series of PCR product of known concentration. GAPDH standard target was diluted in a 10-fold series dilution from 10 nM to 1 pM. These diluted products were qPCR-amplified in two separate reactions stopped at 15 and 18 cycles respectively. The double stranded DNA products were denatured through a modified heat and shook cooling denaturation approach as described previously (Rizzi et al., 2017). Briefly, the samples were denatured for 10 minutes at 95°C and shock-cooled for 5 min in ice to slow down re-hybridization. 120 μL of each of the denatured samples were injected on to separate chips, and allowed to hybridize to the DNA probes on the chip for 1 hour at 37°C. The chips were then washed twice with washing buffer (10mM NaCl in Tris EDTA) to remove unbound DNA. After measuring 2 min of baseline signal, 50 μL of streptavidin magnetic nanoparticles (MNPs) (Miltenyi Biotec) were added in the sample well and the binding signal was measured until the GMR signal reached a plateau, indicating binding saturation. This was roughly between 15–30 minutes for each sample.

2.6 GMR Signal Acquisition.

DNA hybridization causes MNPs to bind to the sensor surface that lead to a change in the measured magnetoresistive (MR) ratio of the sensor. The MR ratio was measured as described previously (Rizzi et al., 2017). Briefly, sensors were biased with a frequency of either f_1=480 Hz or 500 Hz, and an alternating magnetic field of amplitude 3 mT with frequency of f_2=90 Hz was supplied by an external Helmholtz coil. Upon DNA hybridization, magnetized MNPs generate a field measured at $f_1 + f_2$. The measured MR

ratio is the ratio of signals measured at $f_1 + f_2$ and f_1. The DNA binding signal mentioned in 2.5 is measured in terms of $\Delta MR = MR - MR_0$, where MR_0 represents the MR ratio before MNP addition. A National Instruments NI-6259 data acquisition card, containing an 18-bit analog to digital converter, digitizes the binding signal and interfaces with LabVIEW to generate readable results (Hall et. al., 2010).

3. Results

We aim to assess GMR sensors capabilities for quantifying gene expression by detecting biotinylated GAPDH PCR products after reverse transcription and targeted amplification (Fig. 1). To develop the GMR platform for gene expression analysis, series dilutions of GAPDH synthetic DNA were qPCR-amplified to study the dependency of product concentration on the amplification parameters. Afterwards, PCR and GMR were combined to test GMR detection limits for DNA that was qPCR-amplified at varying cycle numbers, to determine the accuracy of GMR for cDNA quantification.

3.1 PCR amplification for varying initial concentrations (c_i) of DNA.

A ten-fold dilution series of GAPDH ssDNA standard from 10 nM to 0.1 pM was qPCR-amplified for 40 cycles, along with total cDNA isolated from a HeLa cell line. The normalized intensity (I) values for each initial concentration (c_i) was extracted and plotted (Fig. 2A) against qPCR cycle number. In Fig. 2B, the normalized intensity values for varying cycle numbers was extracted and plotted against each c_i. The sigmoid function $intensity\,(I) = 1 - \frac{1}{1 + \left(\frac{c_i}{c_o}\right)^p}$ was fitted to the data with p and c_0 free fitting parameters (see supplementary Table S2). Fig. 2B shows fitting results and 95% confidence intervals. All fittings had $R^2 = 0.99$. The results for 15 and 18 cycles offer a broader detectable dynamic range (4 orders of magnitude). The window of the dynamic range depends on the cycle number.

3.2 qPCR Standard Curve Analysis.

The 40-cycle amplification data for both the ssDNA standard and the HeLa cell line DNA was used as described in 3.1; the Cq values were isolated and plotted for the various initial concentrations (c_i). From the Cq values of the diluted ssDNA standard, a standard curve was developed with a linear fit through the semi-logarithmic data, which had a 77.6% efficiency, an R^2 value of 0.994, a slope of −4.007, and a y intercept of −27.594. The average concentration of the HeLa cDNA was determined to be 6.0 ± 0.8 pM after fitting to the standard curve (Fig. 3).

3.3 GMR Signal from varying target initial concentrations (c_i).

GAPDH ssDNA standard target was diluted in a 10-fold series from 10 nM to 1 pM. These diluted products were aliquoted and qPCR-amplified in two separate reactions interrupted at 15 and 18 cycles respectively. Each dilution and cycle number condition was run in duplicate. The fluorescence intensities of the qPCR reaction are shown in Fig. 4A (15 cycle reaction) and Fig. 4B (18 cycle reaction). In Fig. 4A, 1pM could not be detected in the

fluorescence signal, indicating that 0.01 nM is the limit of detection for 15-cycle PCR with a fluorescence readout. In Fig. 4B, the dilution series was extended down to 0.1 pM; however, 0.1 pM could not be detected in the fluorescence signal, indicating that 1 pM is the limit of detection for 18-cycle PCR with a fluorescence readout. From each PCR reaction, 10μL of PCR product was diluted with 190μL of hybridization buffer and hybridized to GMR chips to measure the corresponding GMR signal. A no-template control (no GAPDH DNA, but GAPDH primers, master mix, and DNA suspension buffer) at 18-cycles was also measured to determine the limit of detection of the GMR system.

Fig. 4C and 4D show GMR values measured for varying initial concentration (pre-PCR) $c_{i,}$ along with cell line DNA, after 15-cycle and 18-cycle amplification, respectively. Error bars indicate the standard deviation between the 32 functionalized sensors, with negative reference signal subtracted from all measured values. A linear regression was applied to the semi-logarithmic data, indicating that GMR signal varies linearly with pre-PCR concentration, as each of these concentrations reached a different final concentration c_f post-PCR that could be detected by GMR.

For the 15-cycle linear fit, the slope is 520 (± 60), and the intercept is 1988 (± 107), with an $R^2 = 0.95$; values in parentheses represent 95% confidence intervals (Supplementary Table S3). The cell line DNA amplified 15 cycles gave a GMR signal of 805 (± 95) ppm from which we can calculate the initial concentration to be $c_i = 5.3 \pm 0.3$ pM that is in good agreement with qPCR estimated initial concentration of 6.0 ± 0.8 pM (Fig. 3). The dynamic range is roughly 4 orders of magnitude, and the limit of detection is 1 pM.

For 18-cycle amplification, only concentrations from 1pM to 1nM were fit linearly, as this was the working dynamic range, and values above and below these concentrations gave saturated GMR signal. The slope is 510 (± 10), and the intercept is 2160 (± 34), with an $R^2 = 0.95$; values in parentheses represent 95% confidence intervals (Supplementary Table S3). The cell line DNA amplified 18 cycles gave a GMR signal of 1100 (± 130) ppm from which we can calculate the initial concentration to be $c_i = 8.3 \pm 4.6$ pM that is in good agreement with qPCR estimated initial concentration of 6.0 ± 0.8 pM (Fig. 3). The dynamic range is roughly 4 orders of magnitude, and the limit of detection is 0.1 pM. The no-template control gave little discernable signal, which is represented by a dashed line in both plots. Importantly, 18-cycle amplification gave a limit of detection that was one order of magnitude greater than 15-cycle amplification, as expected.

4. Discussion

The GMR platform has potential as a quantitative gene expression analysis tool. First, 15 and 18-cycle synthetic PCR products at various starting concentrations were shown to each have a dynamic range of 4 orders of magnitude on the GMR. The 15-cycle product had a limit of detection of 1 pM, and 18-cycle product had a limit of detection of 0.1 pM. Although these concentrations would be discernable if qPCR-amplified for more cycles, neither of these concentrations were detectable through the fluorescence signal seen in Fig. 4A (15 cycles) and 4B (18 cycles), highlighting the sensitivity of the GMR platform. Second, the qPCR standard curve showed a starting concentration of 6.0 ± 0.8 pM for the

HeLa cDNA after fitting to the Cq values of the standards (Fig. 3). This result was confirmed in both Fig. 4C and 4D, in which the starting concentration of the HeLa cDNA was determined to be 5.3 ± 0.3, pM and 8.3 ± 4.6 pM, respectively. This result emphasizes that the GMR can measure concentration levels with accuracy comparable to the qPCR.

The findings above demonstrate that the GMR platform can be used for endpoint detection to quantify the starting concentration of PCR products. It has previously been shown that the GMR DNA array has a dynamic detection range from 40 pM to 40 nM (Rizzi et al., 2017). However, this range was established using a synthetic ssDNA sequence with no PCR amplification. To increase the sensitivity of endpoint detection, we have introduced PCR amplification, and have shown that the GMR limit of detection can be brought down to 0.1 pM with 18-cycle PCR amplification (Fig. 4D). PCR amplification is useful to increase GMR sensitivity to low copy numbers, which is beneficial for gene expression analysis, where many transcripts are present in low abundance.

We have shown that PCR amplification provides another degree of freedom (cycle number), which can be tuned to shift the dynamic range of GMR detection. While the low concentration transcripts are better detected on the GMR after 18-cycle amplification (limit of detection at 0.1 pM), high concentration transcripts (10 nM) show signal saturation. Conversely, the 15-cycle amplified product had a higher detection limit on the GMR (1 pM), but provided quantitative detection at high transcript concentrations. These results suggest that 15-cycle amplification on GMR is better for detection of a broader range of concentrations, whereas 18-cycle amplification on GMR might be more suited to enrich for low concentration transcripts.

Not only is the GMR system advantageous for detection of a broad range of transcript concentrations, but also its multiplexing capabilities allow for detection of many genes in parallel. This provides potential for measurement of a gene expression signature in both transcript detection and quantification.

5. Conclusions

The GMR platform provides a dynamic range of 4 orders of magnitude and a limit of detection of 1 pM and 0.1 pM respectively for 15 and 18-cycle amplified products. Cell-line DNA was shown to have a starting concentration of 6.0 ± 0.8 pM through qPCR standard curve analysis, which was subsequently confirmed with GMR analysis. For the first time, this work shows the characterization and quantification of cDNA on the GMR platform, demonstrating the prospective of the GMR to detect multiple mRNA transcripts expressed at different levels. Although the additional step of PCR amplification increases time for analysis, it augments the sensitivity of the GMR bioassay to lower copy numbers. Future work involves amplifying cell line DNA with different primers corresponding to a genetic signature of a particular disease; then transcript concentration can be assessed in multiplex with GMR. Ultimately, the GMR shows potential to be a useful technology in facilitating rapid, point-of-care disease diagnostics.

Supplementary Material

Refer to Web version on PubMed Central for supplementary material.

Acknowledgements

We would like to acknowledge Jared Nesvet for help in qPCR analysis. N.R. acknowledges support from the Stanford Graduate Fellowship. P.C. was supported by NIH T32 training grant [2T32AR050942–06A1] and the Novo Nordisk Senior Postdoctoral Fellowship. This work was supported by NIAID [R01AI125197] and the Autoimmunity center of excellence [U19AI110491].

References

1. Allison DB, Cui X, Page GP, Sabripour M, 2006 Microarray data analysis: from disarray to consolidation and consensus. Nature Reviews Genetics 7, 55–65. 10.1038/nrg1749
2. Andres-Terre M, McGuire HM, Pouliot Y, Bongen E, Sweeney TE, Tato CM, Khatri P, 2015 Integrated, Multi-cohort Analysis Identifies Conserved Transcriptional Signatures across Multiple Respiratory Viruses. Immunity 43, 1199–1211. 10.1016/j.immuni.2015.11.003 [PubMed: 26682989]
3. Arts P, van der Raadt J, van Gestel SHC, Steehouwer M, Shendure J, Hoischen A, Albers CA, 2017 Quantification of differential gene expression by multiplexed targeted resequencing of cDNA. Nature Communications 8, 15190 10.1038/ncomms15190
4. Choi J, Gani AW, Bechstein DJB, Lee J-R, Utz PJ, Wang SX, 2016 Portable, one-step, and rapid GMR biosensor platform with smartphone interface. Biosensors and Bioelectronics 85, 1–7. 10.1016/j.bios.2016.04.046 [PubMed: 27148826]
5. Dobnik D, Štebih D, Blejec A, Morisset D, Žel J, 2016 Multiplex quantification of four DNA targets in one reaction with Bio-Rad droplet digital PCR system for GMO detection. Scientific Reports 6 10.1038/srep35451
6. Elashoff MR, Wingrove JA, Beineke P, Daniels SE, Tingley WG, Rosenberg S, Voros S, Kraus WE, Ginsburg GS, Schwartz RS, Ellis SG, Tahirkheli N, Waksman R, McPherson J, Lansky AJ, Topol EJ, 2011 Development of a blood-based gene expression algorithm for assessment of obstructive coronary artery disease in non-diabetic patients. BMC Medical Genomics 4 10.1186/1755-8794-4-26
7. Gaster RS, Hall DA, Nielsen CH, Osterfeld SJ, Yu H, Mach KE, Wilson RJ, Murmann B, Liao JC, Gambhir SS, Wang SX, 2009 Matrix-insensitive protein assays push the limits of biosensors in medicine. Nature Medicine 15, 1327–1332. 10.1038/nm.2032
8. Hall DA, Gaster RS, Lin T, Osterfeld SJ, Han S, Murmann B, Wang SX, 2010 GMR biosensor arrays: A system perspective. Biosens. Bioelectron 25, 2051–2057. 10.1016/j.bios.2010.01.038 [PubMed: 20207130]
9. Kozera B, Rapacz M, 2013 Reference genes in real-time PCR. Journal of Applied Genetics 54, 391–406. 10.1007/s13353-013-0173-x [PubMed: 24078518]
10. Lee J-R, Haddon DJ, Wand HE, Price JV, Diep VK, Hall DA, Petri M, Baechler EC, Balboni IM, Utz PJ, Wang SX, 2016 Multiplex giant magnetoresistive biosensor microarrays identify interferon-associated autoantibodies in systemic lupus erythematosus. Scientific Reports 6 10.1038/srep27623
11. Maertzdorf J, McEwen G, Weiner J, Tian S, Lader E, Schriek U, Mayanja-Kizza H, Ota M, Kenneth J, Kaufmann SH, 2016 Concise gene signature for point-of-care classification of tuberculosis. EMBO Molecular Medicine 8, 86–95. 10.15252/emmm.201505790 [PubMed: 26682570]
12. Ng E, Nadeau KC, Wang SX, 2016 Giant magnetoresistive sensor array for sensitive and specific multiplexed food allergen detection. Biosensors and Bioelectronics 80, 359–365. 10.1016/j.bios.2016.02.002 [PubMed: 26859787]
13. Osterfeld SJ, Yu H, Gaster RS, Caramuta S, Xu L, Han S-J, Hall DA, Wilson RJ, Sun S, White RL, Davis RW, Pourmand N, Wang SX, 2008 Multiplex protein assays based on real-time magnetic

nanotag sensing. Proceedings of the National Academy of Sciences 105, 20637–20640. 10.1073/pnas.0810822105

14. Rizzi G, Lee J-R, Dahl C, Guldberg P, Dufva M, Wang SX, Hansen MF, 2017a Simultaneous Profiling of DNA Mutation and Methylation by Melting Analysis Using Magnetoresistive Biosensor Array. ACS Nano 11, 8864–8870. 10.1021/acsnano.7b03053 [PubMed: 28832112]
15. Rizzi G, Lee J-R, Guldberg P, Dufva M, Wang SX, Hansen MF, 2017b Denaturation strategies for detection of double stranded PCR products on GMR magnetic biosensor array. Biosensors and Bioelectronics 93, 155–160. 10.1016/j.bios.2016.09.031 [PubMed: 27650710]
16. Xu L, Yu H, Akhras MS, Han S-J, Osterfeld S, White RL, Pourmand N, Wang SX, 2008 Giant magnetoresistive biochip for DNA detection and HPV genotyping. Biosensors and Bioelectronics 24, 99–103. 10.1016/j.bios.2008.03.030 [PubMed: 18457945]
17. Zhao S, Fung-Leung W-P, Bittner A, Ngo K, Liu X, 2014 Comparison of RNA-Seq and Microarray in Transcriptome Profiling of Activated T Cells. PLoS ONE 9, e78644 10.1371/journal.pone.0078644 [PubMed: 24454679]

Highlights:

- GMR platform has dynamic range of 4 orders of magnitude for 18-cycle PCR amplified product.
- GMR platform has 0.1 pM limit of detection for 18-cycle PCR amplified product.
- GMR can measure cDNA concentration levels with accuracy comparable to the qPCR.

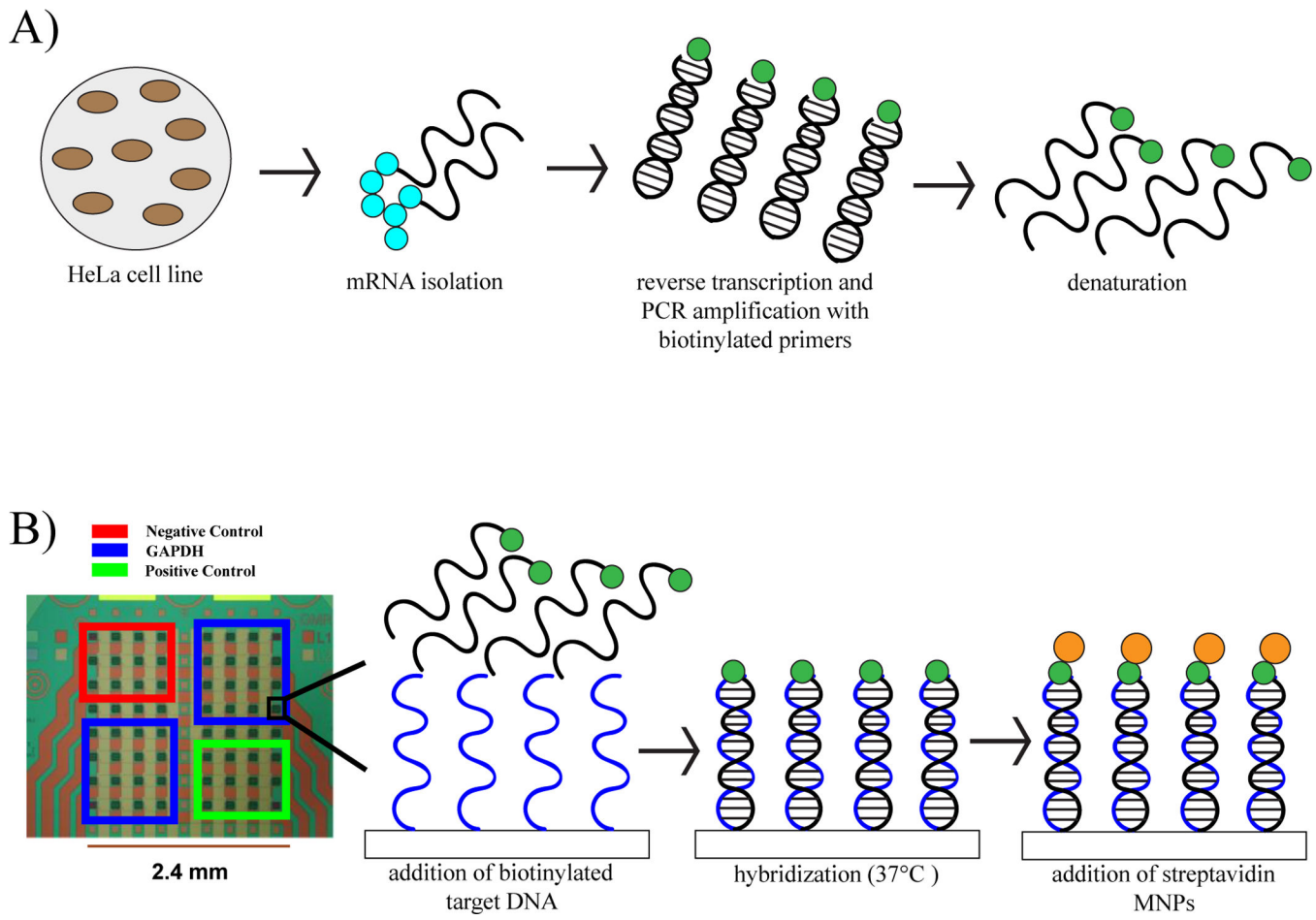

Figure 1.

A) Target DNA preparation. HeLa mRNA was reverse transcribed and PCR-amplified to cDNA with biotinylated GAPDH primers. PCR product was denatured in 95°C to create target ssDNA. **B)** Sensors on the GMR chip are spotted with a GAPDH, negative control, and positive control, according to the spotting pattern seen. GAPDH sensor is functionalized with DNA probes complementary to the GAPDH target ssDNA in (A). This target ssDNA is added to the sensor surface and allowed to hybridize. Signal is measured after adding streptavidin MNPs.

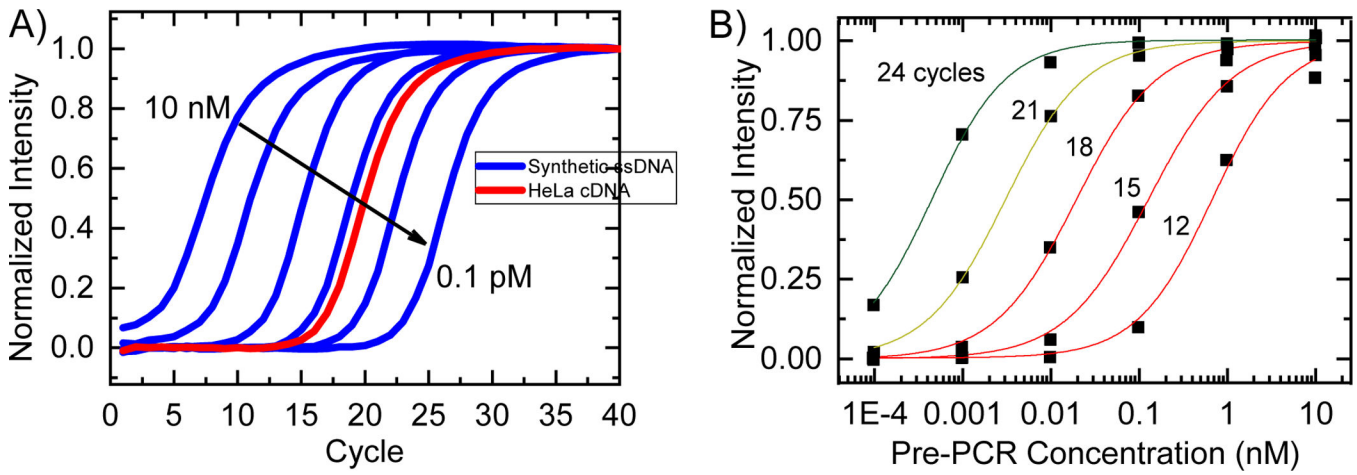

Figure 2.

A). 40-cycle amplification curves for both GAPDH standard ssDNA diluted down in a 10x series dilution and HeLa cDNA amplified with GAPDH primers. **B)** The intensity values (y-axis) from the GAPDH standards in (A) were extracted and plotted for respective cycle numbers (x-axis), and fit to sigmoid functions. Both 15 and 18 cycles gave the largest working range of detection (4 orders of magnitude).

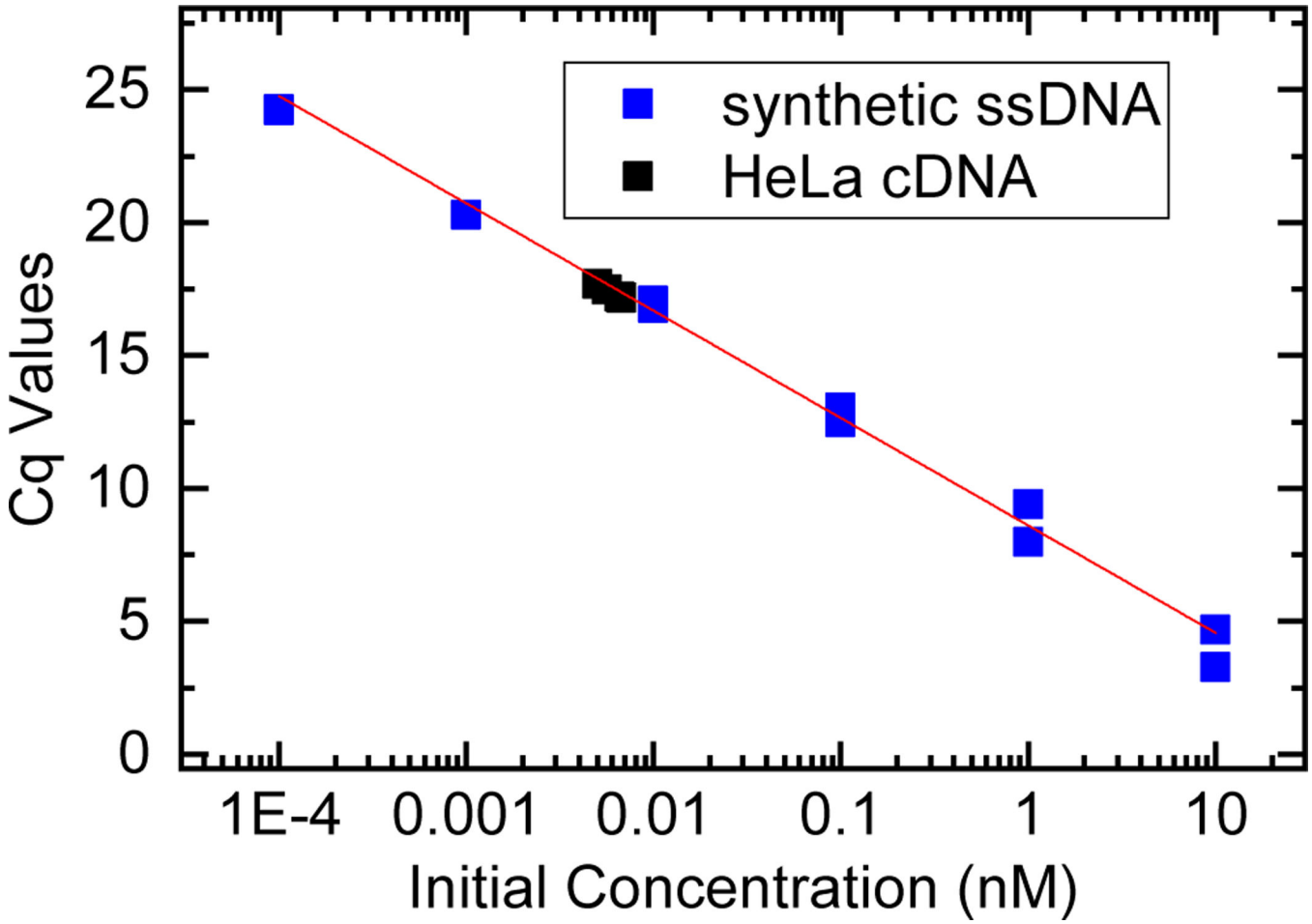

Figure 3.

qPCR standard curve plotted for varying concentrations of synthetic GAPDH DNA. The data were fit to a linear function, with an efficiency of 77.6%, an R^2 value of 0.994, a slope of −4.007, and a y intercept of −27.594. The average concentration of the HeLa cDNA was determined to be 6.0 ± 0.8 pM after fitting to the standard curve.

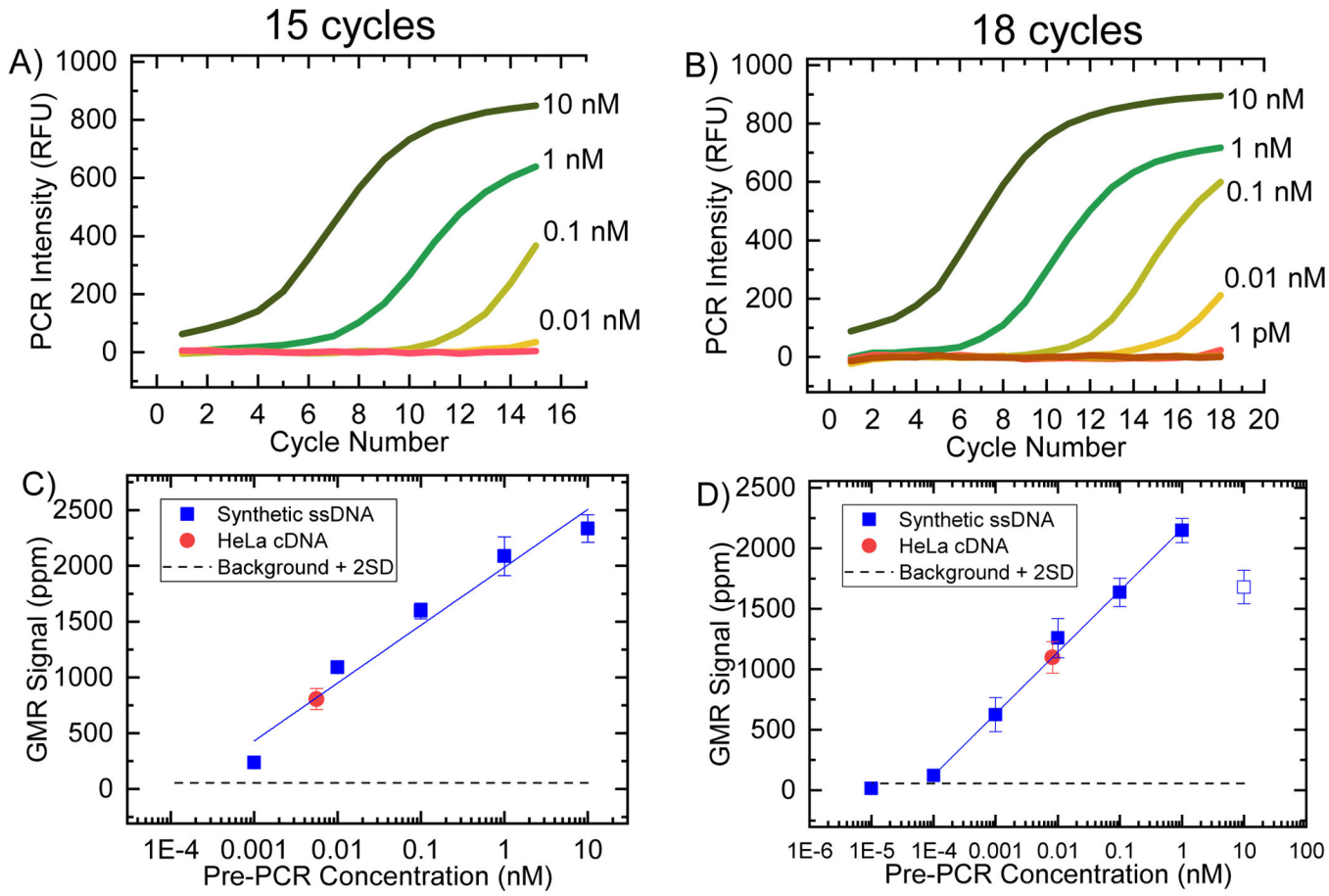

Figure 4.

A) GAPDH standard was diluted down pre-PCR 10x in a series dilution (10 nM→ 1 pM) and then PCR amplified for 15 cycles. 0.01 nM is the qPCR limit of detection; 1 pM showed no amplification. **B)** GAPDH standard was diluted down pre-PCR 10x in a series dilution (10 nM→ 0.1 pM) and then PCR amplified for 18 cycles. 1 pM is the qPCR limit of detection; 0.1 pM showed no amplification. **C)** 15-cycle PCR product was added to different GMR chips and allowed to hybridize for 1 hour. Data was fit to a semi-logarithmic trendline, showing a working range of 4 orders of magnitude (1 pM→10nM), with a limit of detection of 1 pM. **D)** 18-cycle PCR product was added to different GMR chips and allowed to hybridize for 1 hour. Data was fit to a semi-logarithmic trendline, showing a working range of 4 orders of magnitude (0.1 pM→1 nM), with a limit of detection of 0.1 pM. The signal recorded at 10 nM represents an outlier; this point is out of the 18-cycle dynamic range. For both (C) and (D), points represents the mean GMR signal saturation level for the 32 GAPDH sensors, normalized to the mean negative control signal. Error bars indicate standard deviation in GAPDH signal between the 32 GAPDH sensors. Background line indicates the GMR signal measured from the no-template control.